
Human Interpretable AI: Enhancing Tsetlin Machine Stochasticity with Drop Clause

Jivitesh Sharma*

Center for Artificial Intelligence Research
 Department of ICT
 University of Agder
 Grimstad 4879, Norway
 jivitesh.sharma@uia.no

Rohan Kumar Yadav

Center for Artificial Intelligence Research
 Department of ICT
 University of Agder
 Grimstad 4879, Norway
 rohan.k.yadav@uia.no

Ole-Christoffer Granmo

Center for Artificial Intelligence Research
 Department of ICT
 University of Agder
 Grimstad 4879, Norway
 ole.granmo@uia.no

Lei Jiao

Center for Artificial Intelligence Research
 Department of ICT
 University of Agder
 Grimstad 4879, Norway
 lei.jiao@uia.no

Abstract

In this article, we introduce a novel variant of the Tsetlin machine (TM) that randomly drops clauses, the key learning elements of a TM. In effect, TM with drop clause ignores a random selection of the clauses in each epoch, selected according to a predefined probability. In this way, additional stochasticity is introduced in the learning phase of TM. Along with producing more distinct and well-structured patterns that improve the performance, we also show that dropping clauses increases learning robustness. To explore the effects clause dropping has on accuracy, training time, and interpretability, we conduct extensive experiments on various benchmark datasets in natural language processing (NLP) (IMDb and SST2) as well as computer vision (MNIST and CIFAR10). In brief, we observe from +2% to +4% increase in accuracy and 2 \times to 4 \times faster learning. We further employ the Convolutional TM to document interpretable results on the CIFAR10 dataset. To the best of our knowledge, this is the first time an interpretable machine learning algorithm has been used to produce pixel-level human-interpretable results on CIFAR10. Also, unlike previous interpretable methods that focus on attention visualisation or gradient interpretability, we show that the TM is a more general interpretable method. That is, by producing rule-based propositional logic expressions that are *human*-interpretable, the TM can explain how it classifies a particular instance at the pixel level for computer vision and at the word level for NLP.

1 Introduction

Researchers across various fields are increasingly paying attention to the interpretability of AI techniques. While interpretability previously was inherent in most machine learning approaches, state-of-the-art methods now increasingly rely on black-box deep neural network-based models. Natively, these can neither be interpreted during the learning stage nor while producing outputs. For this rea-

*Corresponding author. Email: jivitesh.sharma@uia.no

son, a surge of techniques attempts to open the black box by visual explanations and gradient-based interpretability [6, 8, 10, 26, 30, 33, 35, 39, 45].

However, current neural network interpretation techniques are approximate and incomplete. For instance, gradient-based interpretation only provides visual maps that capture maximum activation. Such activation is not truly interpretable because the activation does not explain how the model reasons. Instead, the activation merely shows where the network is paying attention [32]. Indeed, the interpretability of neural networks is quite fragile [13]. Small perturbations in the input can completely change the interpretation of the neural network. In particular, attention-based models have outperformed most other natural language processing approaches [5, 11, 29]. Yet, attention-based interpretability relies on visualizing attention weights [34]. Like gradient visualization, attention weight visualization does not adequately explain how the model comes to a decision [16]. Due to the difficulties of interpreting black-box models, researchers have argued that one should abandon such approaches altogether and instead adopt inherently interpretable models [32].

The Tsetlin Machine (TM) is a natively interpretable pattern recognition algorithm that produces logical rules [14]. Despite being logic-based, the TM is a universal function approximator, like a neural network. In brief, it employs an ensemble of Tsetlin Automata (TA) that learns propositional logic expressions from Boolean (propositional) input features. Each TA decides whether to include a specific Boolean input feature in an AND-pattern, either as-is or negated. In this way, the TM performs feature selection innately. Due to its Boolean representations and finite-state automata learning mechanisms, it has a minimalistic memory footprint. Propositional logic drives learning, eliminating the need for floating-point operations. More importantly, TM achieves human-level interpretability by leveraging sparse disjunctive normal form. Indeed, humans are particularly good at understanding flat and short logical AND-rules, reflecting human reasoning [28].

Paper Contributions. For some datasets it turns out that the vanilla TM is prone to overfitting, and the TM currently lacks the powerful regularization techniques available for neural networks. To address this challenge, in this article we propose a novel TM scheme called *drop clause*, inspired by dropout in neural networks [37]. We further explore the effects drop clause has on TM performance in various benchmark datasets from natural language processing (NLP) and computer vision. We first look at how drop clause changes the structure of clauses and their ability to capture unique and robust patterns. We also investigate pixel level interpretability on the CIFAR-10 dataset [19]. To the best of our knowledge, this is the first time pixel-level human interpretable results have been reported on the CIFAR-10 dataset. Apart from this, we also compare the interpretability of patterns captured by clauses with and without dropout on NLP sentiment analysis tasks. Finally, drop clause enables faster training. We list the contributions of this paper below.

1. We propose to drop clauses randomly during each training iteration, which introduces additional stochasticity in the model.
2. We demonstrate that with drop clause, the TM captures more unique patterns that boost its performance.
3. We show competitive results with other related models on natural language sentiment analysis and image classification.
4. We report human-interpretable results on natural language processing and computer vision tasks.
5. Apart from performance benefits, the TM has very low memory consumption as it works on Boolean data only and does not need any floating point operations. These advantages are amplified by drop clause.
6. We show that the convergence analysis for the TM also holds for the drop clause version.
7. To the best of our knowledge, we show pixel-level human-interpretable results on the CIFAR-10 dataset for the first time.

Paper Organization. The rest of the paper is laid out as follows: Section 2 covers notable contributions to the field of interpretable AI, while Section 3 describes our proposed drop clause method in detail. Section 4 then presents the results from our NLP and computer vision experiments, focusing on accuracy, interpretability, and computation time. Section 5 shows some limitations of our model and Section 6 concludes our paper.

2 Interpretable AI: Related Work

There has been a surge of research in interpretable AI. Most of the studies focus on making neural networks more interpretable. Currently, state-of-the-art techniques use visual explanations and gradient interpretability. We briefly discuss selected related studies in this section. One approach is to compute the gradients of the class scores for an input image to visualize which parts of the input image impact the classification [35]. Another approach to visualize class-specific score maps is introduced in [45]. The technique forces each filter in the top convolutional layers to learn a class-specific object by adding a modified mutual information loss. Training is end-to-end by adding the local filter loss to the task-specific loss. These steps produce a map of interest for the top convolutional layers. In [30], the authors propose a two-stage approach. The first stage learns to estimate the conditional probability distribution of patches of pixels separately. The second stage, in turn, averages these estimates to obtain a global assessment. The Grad-CAM method, proposed in [33], has been widely employed to visualize CNN outputs. Grad-CAM uses the gradients of a target class from the final convolution layer to produce a coarse localization map. The map highlights the regions in the image used by the neural network for predicting the concept. The work in [6] analyses how different layers, training conditions, model architecture, layer width, and accuracy impact visual interpretability. Similar to convolutions, Saak transform extracts interpretable features that capture distinct feature regions of the image [26].

NLP model interpretation methods largely visualize attention weights for words. Example models include BERT and contextualized embedding [5, 11, 29], which capture the semantic relatedness among words using context. However, the weights assigned by the attention vector to each input do not necessarily provide a faithful explanation of classification [16, 34].

Overall, state-of-the-art methods use feature importance maps for interpretation, both for computer vision- and NLP models. These maps only show where the neural network is “looking”. Such an approach is not truly interpretable because one does not explain why attention is where it is. Many researchers have attempted to replicate more human-level interpretation behavior in neural networks [22], but have largely failed so far. In this paper, we improve the performance of the TM by introducing a novel method called drop clause. We also evaluate its convergence, accuracy, computation time, and interpretability. Additionally, we show how the human-interpretable clauses straightforwardly map to classification decisions, both in NLP and computer vision.

3 Drop Clause for Tsetlin Machines

As discussed in the previous section, neural networks are difficult to interpret. Therefore, applications leverage them as black boxes, with the adverse effects that entail. However, for high-stakes applications, such as healthcare, black-box approaches are not sufficient. Modern society needs reliable, unbiased, and trustworthy AI systems. Researchers have shown that neural networks are not fully mature for integration into society. For example, neural network interpretability is fragile towards adversarial examples [13]. Generating adversarial perturbations that produce visually indistinguishable images for humans leads to dramatically different neural network interpretations, without changing the label.

In addition, it is argued in [32], that neural networks are black boxes that cannot be fully explained. There were several arguments opposing the use of explainability on black box models and employing inherently interpretable models. Also [32] suggests, the machine learning community faces three algorithmic challenges to succeed with human-level interpretability. Although neural networks are inherently inadequate for these challenges, the TM addresses them natively:

1. *Challenge 1: Rule-based logical models* - The TM learns a rule-based model using logical operations. Learning is game-theoretic with Nash equilibria that correspond to the optimal propositional logic expressions [14, 18, 46].
2. *Challenge 2: Linear models with sparse scoring systems* - The TM is a linear model that produces sparse clauses and integer weighted scores [3].
3. *Challenge 3: Domain-specific interpretable AI* - The TM is inherently interpretable, used for producing interpretable models across several domains [2, 7, 21, 43].

In this section, we first briefly present the basic TM as well as the convolutional version. Thereafter, we introduce the details of our drop clause technique, which enhances the stochasticity of TM learning. Our goal is to reduce overfitting behaviour and considerably increase performance. We also show pixel-level human interpretability on CIFAR-10 and word-level human interpretability on SST2. And, as the TM is based on Boolean data and propositional logic, it has very low memory footprint and computational complexity (*zero FLOPs*).

3.1 TM and Convolutional TM

A TM in its simplest form takes a feature vector $\mathbf{x} = [x_1, x_2, \dots, x_o] \in \{0, 1\}^o$ of o Boolean values as input, producing a Boolean output $\hat{y} \in \{0, 1\}$ [14]. Patterns are expressed as conjunctive clauses (AND-rules), built from literals $L = \{l_1, l_2, \dots, l_{2o}\} = \{x_1, x_2, \dots, x_o, \neg x_1, \neg x_2, \dots, \neg x_o\}$:

$$\hat{y} = 0 \leq \sum_{j=1,3,\dots}^{n-1} \bigwedge_{k=1}^{2o} [g(a_k^j) \Rightarrow l_k] - \sum_{j=2,4,\dots}^n \bigwedge_{k=1}^{2o} [g(a_k^j) \Rightarrow l_k]. \quad (1)$$

Above, a_k^j is the TA state that controls inclusion of literal l_k in clause j and $g(\cdot)$ maps the TA state to action 0 or 1. The imply operator, in turn, implements the action in the clause. Even-indexed/odd-indexed clauses vote for output $\hat{y} = 0/\hat{y} = 1$. A detailed explanation can be found in the Appendix A.1.

The Convolutional TM (CTM) is as an interpretable alternative to CNNs [15]. Whereas the TM categorizes an image by employing each clause once to the whole image, the CTM uses each clause as a convolution filter. That is, a clause is evaluated multiple times, once per image patch taking part in the convolution. The output of a convolution clause is obtained simply by ORing the outcome of evaluating the clause on each patch:

$$\hat{y} = 0 \leq \sum_{j=1,3,\dots}^{n-1} \bigvee_{b=1}^B \left[\bigwedge_{k=1}^{2o} [g(a_k^j) \Rightarrow l_k^b] \right] - \sum_{j=2,4,\dots}^n \bigvee_{b=1}^B \left[\bigwedge_{k=1}^{2o} [g(a_k^j) \Rightarrow l_k^b] \right]. \quad (2)$$

Here, b refers to one out of B available image patches [15]. See Appendix A.2 for further details.

3.2 Drop Clause

Although there might be an enormous amount of patterns in real-life data, with a sufficient number of clauses the TM can identify the most important ones. However, patterns might differ between training and testing data, leading to TM overfitting. We therefore propose a novel regularization method for the TM called drop clause. This technique is inspired by the dropout method for neural networks. In drop clause, clauses are removed with a probability p in each training epoch:

$$\hat{y} = 0 \leq \sum_{j=1,3,\dots}^{n-1} \pi_j \bigwedge_{k=1}^{2o} [g(a_k^j) \Rightarrow l_k] - \sum_{j=2,4,\dots}^n \pi_j \bigwedge_{k=1}^{2o} [g(a_k^j) \Rightarrow l_k]. \quad (3)$$

Above, $\pi_j \in \{0, 1\}$ for clause j is zero with probability p for each complete epoch. The purpose is to reduce the chance of learning redundant patterns. The vanilla TM and its drop clause variant are equivalent if $p = 0$.

Drop clause in TM works in a similar way as dropout in neural networks. A basic TM seeks to minimize prediction error on the training data. Achieving this, there may still be unused patterns available in the training data. These patterns can potentially be useful when facing new data, such as test data. By randomly dropping clauses for complete epochs, we mobilize other clauses to take over the role of the dropped clauses. However, due to the stochastic learning, the mobilized clauses may solve the task in a different way. Hence, robustness increases overall when the complete set of clauses are turned on again. These advantages of using drop clause have been shown experimentally in the next section.

The stochasticity induced by the drop clause in the learning process of TM is similar to the stochasticity induced by the stochastic gradient descent (SGD) [31]. In SGD, a mini-batch of training samples is selected randomly from the training data. While, in drop clause, various sets of clauses are selected for training with probability $1 - p$. The major difference is that, SGD is stochastic in terms

of data sampling during the learning stage, whereas drop clause is stochastic in terms of sampling the elements of the model structure (clauses are the elements that form the TM model). Another difference is that the stochasticity of drop clause can be adjusted with the drop clause probability hyper-parameter p .

4 Experiments and Results

We here investigate the effects drop clause has on the accuracy, training time, and interpretability of TMs. To assess the generality of our approach, we test drop clause both on natural language sentiment analysis and image classification. For natural language sentiment analysis, we use TM with weighted clauses [3], and for image classification, we use the CTM unless otherwise mentioned. We also compare the drop clause approach with other related interpretable and explainable models. We implement the drop clause version of the TM on top of a parallel GPU implementation using PyCUDA. We run our models on 16 NVIDIA Tesla V100 TensorCore GPUs.

4.1 Natural Language Sentiment Analysis

We now explore the performance of drop clause on NLP tasks. The first experiments assess how various drop clause probabilities affect the accuracy and then compare the best found configuration with similar state-of-the-art techniques. After that, we study how to interpret the clauses involved in a particular classification, uncovering significant drop clause effects on interpretability. We have used two popular standard evaluation frameworks: the IMDb dataset [25] and Stanford Sentiment Treebank 2 (SST-2) dataset [36].

4.1.1 Results

The TM with drop clause is trained on 10,000 clauses per class, $T = 8,000$, and $s = 5.0$ (the hyper-parameters of a TM, detailed in Appendix A.1) both for IMDb and SST-2. Higher number of clauses than this did not significantly enhance the accuracy. We start with comparing the difference in performance with respect to change in drop clause probability, shown in Table 1. The selected drop clause probabilities are $p : \{0.1, 0.25, 0.5, 0.75\}$. For both datasets, the best performance is achieved with $p = 0.75$, which is equivalent of dropping 75% of the total clauses per class, per epoch. As seen, drop clause has significant effect on accuracy, with average accuracy going up 2.8% for IMDb and 4.58% for SST-2. Additionally, we observe a substantial reduction in training time. With drop clause $p = 0.75$, the training time decreases from 80.25s to 17.1s and 42.15s to 8.5s per epoch on IMDb and SST-2, respectively. Inference times on both these datasets are less than 5ms per sample. Peak accuracy is 90.1% ($\pm 0.3\%$) for IMDb and 81.2% ($\pm 0.4\%$) for SST-2, averaged over 100 runs.

Table 1: Effect of Drop Clause on Natural Language Sentiment Analysis. The upper results show the best reproducible accuracy and lower ones are the mean and standard deviation of the last 25 epochs when running the model hundred times.

TM	$p = 0$	$p = 0.1$	$p = 0.25$	$p = 0.5$	$p = 0.75$
IMDb	87.2 (86.88 ± 0.2)	87.8 (86.90 ± 0.2)	88.6 (87.78 ± 0.5)	89.4 (88.40 ± 0.8)	90.27 (89.90 ± 0.4)
SST-2	76.3 (75.15 ± 1.0)	76.5 (75.20 ± 1.1)	77.9 (76.40 ± 1.2)	79.6 (77.67 ± 1.5)	81.2 (80.04 ± 1.1)

Table 2 collects results from comparable state-of-the-art techniques. These are standard baselines for text classification and interpretable models. As observed, TM without drop clause has lower accuracy compared to the deep neural network based models. Enhanced with drop clause, however, accuracy is comparable. In comparison to a task-oriented word embedding method (ToWE-CBOW), our proposed model outperforms it on SST-2 whereas falls slightly below on IMDb. Another approach is to learn emotional semantics as vectors (Emo2vec), which performs at the same level as TM drop clause on SST-2. There are various attempts to visualize attention maps to interpret NLP models. One approach uses additive attention (AD), which captures the internal mechanism of attention by looking into the gradient update process. This method uses polarity score and attention

score for global assessment of the significance of a text token. While it is disputed whether attention is explanation [16], the approach is significantly outperformed by our proposed model on both the datasets. Note that our model only relies on the word tokens in the target datasets, without considering any additional pretrained world knowledge, like word2vec, Glove and BERT. Yet, it achieves competitive performance compared to accepted baselines and interpretable neural network models. Also, compared to these models, the TM has much lower memory footprint and zero FLOPs.

Table 2: Comparison of TM with state-of-the-art for NLP.

	TM	TM ($p = 0.75$)	LRP [4]	AD [38]	Emo2vec [41]	ToWE-CBOW [23]
IMDb	87.2	90.27	-	88.9	-	90.8
SST-2	76.3	81.2	82.9	80.8	81.2	78.4

4.1.2 Interpretability

We next investigate local model interpretability by using a randomly selected test example from SST-2: "A waste of fearless purity in the acting craft". The example was selected among the ones that were correctly classified with drop clause and incorrectly classified without. The purpose is to contrast how drop clause affects interpretability. Note that for NLP, the majority of the features appear in negated form. In order to have human level understanding of the model, we use frequency-based interpretation, i.e., we highlight the features based on how frequently they appear in clauses, as explained in [44]. An arguable unique property of TMs is that the patterns they produce are both descriptive (frequent) and discriminative. In other words, each clause captures a full description of the target concept, not merely the discrimination boundary.

Figure 1 highlights the top 100 most frequent features in negated form (bright color means high frequency), present in the clauses triggered by the given sample. Three example clauses C_0 , C_2 , and C_4 are shown below the color-coded features. In this case, the prediction is wrong. More importantly, the literals that take part in the conjunctions do not make sense.

The corresponding result for drop clause is depicted in Figure 2. Here, the 100 most frequent features in the negated form seem intuitive for predicting negative sentiment. Features such as "NOT witty (witty)", "NOT grace (graceful)", "NOT terrif (terrific)", "NOT honest", "NOT cool", or "NOT intellig (intelligent)" generally mean absence of positive sentiment for human beings, which in this case makes the model draw the correct conclusion (negative sentiment). Some of the specific patterns that are responsible for predicting the correct output are C_0 , C_2 , and C_4 , as shown in the figure. Although randomly chosen, this example is representative for how TM with drop clause is able to capture a larger variety of correct patterns than what the vanilla TM is capable of.

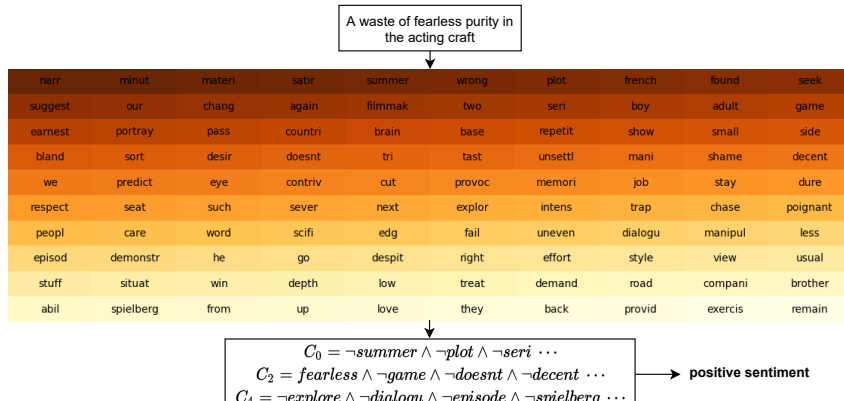


Figure 1: Interpretability of a sample without drop clause.

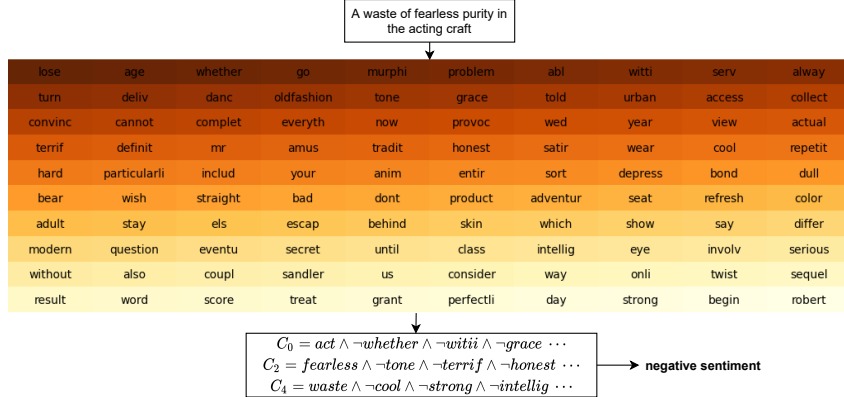


Figure 2: Interpretability of a sample with drop clause.

4.2 Image Classification

We now turn to image classification, again focusing on how drop clause affects accuracy, training time, and interpretability. To this end, we evaluate drop clause on two benchmark image classification datasets: MNIST [20] and CIFAR-10 [19]. In particular, we present pixel-level human-interpretable results for CIFAR-10. We binarize the datasets using an adaptive Gaussian thresholding procedure as proposed in [15]. This binarization results in images with merely 1 bit per pixel per channel.

4.2.1 Results

The CTM configuration for MNIST uses 8,000 clauses per class, $T = 250$, and $s = 5.0$. For CIFAR-10 we employ 60,000 clauses per class, $T = 750$, and $s = 10$. Including additional clauses did not yield any significant performance gain. Again, we explore the effects of four drop clause probability settings, $p : \{0.1, 0.25, 0.5, 0.75\}$, shown in Table 3. The best performance is achieved with $p = 0.25$, which is equivalent to dropping a quarter of the clauses per training iteration. Notice the notable performance increase, especially on CIFAR-10, with drop clause of $p = 0.25$. Peak accuracy on MNIST is 99.45% ($\pm 0.25\%$) and on CIFAR-10 it is 73.1% ($\pm 0.4\%$), averaged over 100 runs².

Apart from the accuracy gain, drop clause with $p = 0.25$ reduces training time by approximately 25%, both for CIFAR-10 and MNIST. For instance, training time per epoch drops from 61.83s to 45.58s for CIFAR-10.

Table 3: Effect of Drop Clause on Image Classification. The upper results show the best reproducible accuracy and the lower ones are the mean and standard deviation of the last 25 epochs when running the model hundred times.

CTM	$p = 0$	$p = 0.1$	$p = 0.25$	$p = 0.5$	$p = 0.75$
MNIST	99.3 (99.12 \pm 0.1)	99.3 (99.15 \pm 0.1)	99.45 (99.30 \pm 0.1)	99.35 (99.20 \pm 0.1)	98.2 (98.07 \pm 0.1)
CIFAR-10	70.1 (69.60 \pm 0.4)	70.5 (69.88 \pm 0.4)	73.1 (72.67 \pm 0.4)	72.6 (71.50 \pm 0.7)	69.6 (68.75 \pm 0.7)

Table 4 contains results from related techniques, contrasted against the CTM results. The SAAK model [26], achieves similar results as drop clause. However, as discussed in Section 2, the resulting visualization maps simply show where the model is looking, and is not truly interpretable. We also compare our model's performance with NODE (Neural Ordinary Differential Equations) [9] and

²We also tested our model on Fashion-MNIST. Our best model achieved 92.2% ($\pm 0.6\%$), averaged over 100 runs, with the same hyperparameters as for MNIST.

ANODE [12], which are continuous depth expressive neural networks. Notice how CTM with drop clause outperforms both NODE and ANODE by a significant margin.

Binary neural networks can be represented exactly as a propositional logic expression [27]. As such, they are particularly comparable to CTM and we therefore also include results for EEV-BNN [17]. EEV-BNN is a binary neural network that has been verified with Boolean satisfiability. The drop clause CTM significantly outperforms EEV-BNN, as shown in Table 4.

The inference time for the drop clause CTM on CIFAR-10 is $1.5ms$ per image, leveraging the computation benefits of only using logical operations for TM inference, and no floating point operations.

Table 4: Comparison on Image Classification

	CTM	CTM ($p = 0.25$)	EEV-BNN [17]	NODE [9]	ANODE [12]	Saak [26]
MNIST	99.3	99.45	97.6	96.4	98.2	99.3
CIFAR-10	70.1	73.1	55.2	53.7	60.6	74.6

4.2.2 Interpretability

In image classification, TM clauses form self-contained patterns by joining pixels into multi-pixel structures. They can therefore be interpreted at the pixel level by humans. That is, the image pixels are inputted directly to the clauses, that are propositional AND-rules, which are relatively easy for humans to comprehend [40]. To the best of our knowledge, this is the first time pixel-level human interpretability has been shown on CIFAR-10.

The CTM forms clauses from the pixels of the square image patches obtained in the convolution. Accordingly, we extract the top k highest weighted clauses per class in patch form. For visualization, we represent the non-negated pixels of a clause as 1.0, negated pixels as -1.0 , and excluded pixels as 0.0. In addition to the image content, each clause also encode at what positions in the image it is valid. If a certain position is invalid, the clause pixel values are treated as 0.0 to indicate no activation at that location. The resulting clause masks are applied over the image and their activation maps are added up to produce a heatmap.

In Figure 3, we compare the heatmaps produced by the vanilla CTM and the CTM with drop clause. As seen, drop clause is able to capture the object more precisely. We believe this is because the remaining clauses are forced to substitute the dropped clauses, learning to perform their tasks. Due to the stochastic nature of the learning, they will, however, learn to perform the tasks differently than the dropped clauses. As a result, drop clause reduces redundancy and induces diversity in the learning of the patterns.

Figure 4 visualizes how the image decomposes into patches and how each patch is represented by multiple clauses. The figure shows how patterns are identified in an image by the clauses in terms of the pixels. In this case, each clause is comprised of an input of 64 pixels in 8×8 patch form. The clauses are formed using these pixels. The pixels are simply joined together by the logical NOT (\neg) and AND (\wedge) operators to form propositional logic expressions. The figure further depicts three patches that have been extracted from different locations in the image. The clause expressions shown in the figure are the ones that are activated in that particular patch for a particular class. Since the clauses are logical AND-rules, localized within the patches, they support pixel-level interpretation facilitating human comprehension [28].

5 Limitations

Drop clause improves the performance of the TM, enhancing the advantages TMs have over neural networks and other interpretable models, in terms of computational complexity, memory consumption, training and inference time, and perhaps most importantly, interpretability. Yet, the TM still achieves lower accuracy on the datasets we use here when compared to the state-of-the-art neural network models. We conjecture that the accuracy gap could be caused by the Booleanization information loss, going from 3×8 bits pixel values to 3 Boolean values (3 bits). Thresholding the 3 color channels separately may also be sub-optimal because the combinations of the three colour channels

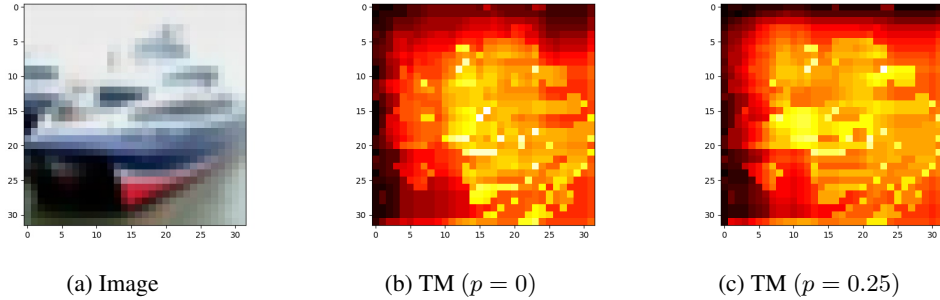


Figure 3: CIFAR-10 Interpretability with and without Drop Clause: (a) represents the actual image, (b) represents the heatmap generated by clause weights of the vanilla TM and (c) represents the heatmap generated by clause weights of the drop clause TM.

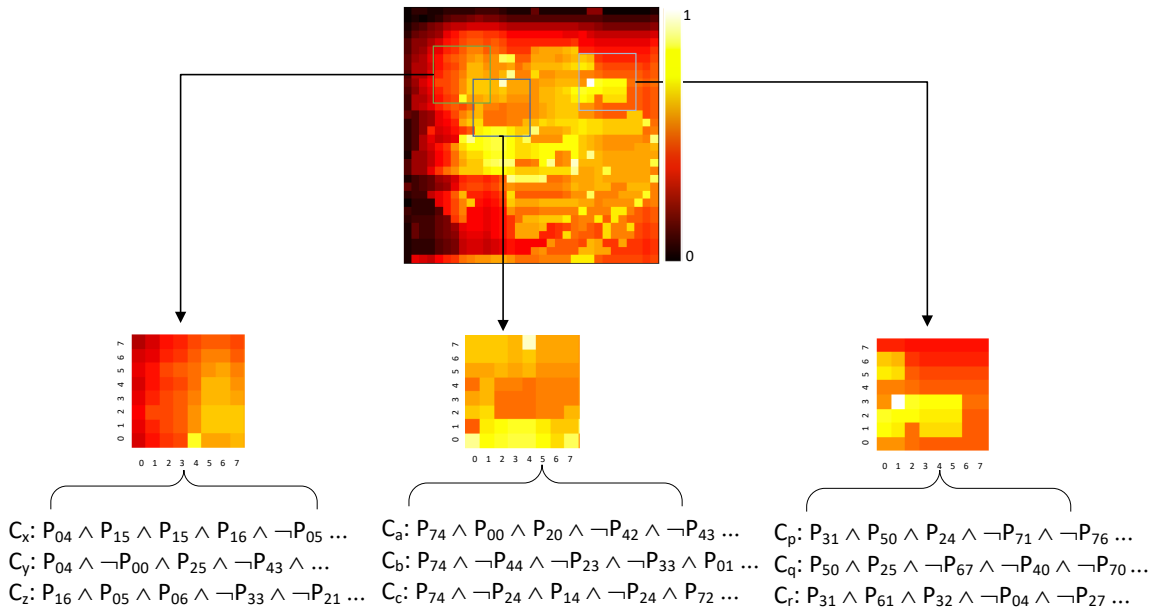


Figure 4: CIFAR-10 Pixel-level Interpretability - Patches of 8×8 are taken at a time. The three clauses shown per patch are some of the top 100 highest weighted clauses for the ship class that have maximum activations in that patch. The pixels shown in the clauses are activated in that patch. Note that, the clauses are longer than shown here.

produce different colours and textures. In brief, how to Booleanize color images in a way suitable for TMs is an open research question. In case of MNIST and Fashion-MNIST, however, images are grey scale. Hence, Booleanization removes less information, and the TM performs on par with neural networks. Another challenge arises in natural language processing tasks. Here, pretrained models have been dominant, leveraging unlabelled data. Important models include word2ve, GloVe, BERT, and GPT. Pre-training usually boosts performance to a significant degree. How to incorporate pre-training in TMs is currently unclear, with the exception of enhancing the input with GloVe-derived synonyms [42]. In addition, TMs require Boolean input, making it difficult to leverage existing high dimensional embeddings, impeding performance.

6 Conclusion

In this paper, we propose *drop clause* as a technique to improve the generalization ability of the TM. Drop clause enhances stochasticity during training, to provide more diverse patterns. As a result, TM performance is significantly boosted on the IMDb and SST-2 datasets for sentiment analysis,

and MNIST and CIFAR-10 for image classification, both in terms of accuracy, training time and interpretability. We also compare our model with other related models, reporting competitive accuracy levels. By visualizing the TM model, we uncover that drop clause patterns seem more robust by being more diverse. We also report pixel-level interpretability on the CIFAR-10 dataset and word-level interpretability on the SST-2 dataset. Further work includes improved Booleanization techniques for color images and self-supervised training of interpretable TM-based language models.

References

- [1] K. Darshana Abeyrathna, Ole-Christoffer Granmo, Xuan Zhang, Lei Jiao, and Morten Goodwin. The Regression Tsetlin Machine - A Novel Approach to Interpretable Non-Linear Regression. *Philosophical Transactions of the Royal Society A*, 378, 2020.
- [2] K. Darshana Abeyrathna, Harsha S. Gardiyawasam Pussewalage, Sasanka N. Ranasinghe, Vladimir A. Oleshchuk, and Ole-Christoffer Granmo. Intrusion Detection with Interpretable Rules Generated Using the Tsetlin Machine. In *2020 IEEE Symposium Series on Computational Intelligence (SSCI)*. IEEE, 2020.
- [3] Kuruge Darshana Abeyrathna, Ole-Christoffer Granmo, and Morten Goodwin. Extending the Tsetlin Machine With Integer-Weighted Clauses for Increased Interpretability. *IEEE Access*, 9, 2021.
- [4] Leila Arras, Grégoire Montavon, Klaus-Robert Müller, and Wojciech Samek. Explaining recurrent neural network predictions in sentiment analysis. In *Proceedings of the 8th Workshop on Computational Approaches to Subjectivity, Sentiment and Social Media Analysis*, pages 159–168, Copenhagen, Denmark, September 2017. Association for Computational Linguistics.
- [5] Dzmitry Bahdanau, Kyunghyun Cho, and Yoshua Bengio. Neural machine translation by jointly learning to align and translate, 2016.
- [6] David Bau, Bolei Zhou, Aditya Khosla, Aude Oliva, and Antonio Torralba. Network dissection: Quantifying interpretability of deep visual representations. *CoRR*, abs/1704.05796, 2017.
- [7] Geir Thore Berge, Ole-Christoffer Granmo, Tor Oddbjørn Tveit, Morten Goodwin, Lei Jiao, and Bernt Viggo Matheussen. Using the Tsetlin Machine to Learn Human-Interpretable Rules for High-Accuracy Text Categorization with Medical Applications. *IEEE Access*, 7:115134–115146, 2019.
- [8] Akhilan Boopathy, Sijia Liu, Gaoyuan Zhang, Cynthia Liu, Pin-Yu Chen, Shiyu Chang, and Luca Daniel. Proper network interpretability helps adversarial robustness in classification, 2020.
- [9] Ricky T. Q. Chen, Yulia Rubanova, Jesse Bettencourt, and David K Duvenaud. Neural ordinary differential equations. In S. Bengio, H. Wallach, H. Larochelle, K. Grauman, N. Cesa-Bianchi, and R. Garnett, editors, *Advances in Neural Information Processing Systems*, volume 31. Curran Associates, Inc., 2018.
- [10] Xi Chen, Yan Duan, Rein Houthooft, John Schulman, Ilya Sutskever, and Pieter Abbeel. Infogan: Interpretable representation learning by information maximizing generative adversarial nets. In *Proceedings of the 30th International Conference on Neural Information Processing Systems, NIPS’16*, page 2180–2188, 2016.
- [11] Jacob Devlin, Ming-Wei Chang, Kenton Lee, and Kristina Toutanova. BERT: Pre-training of deep bidirectional transformers for language understanding. In *Proceedings of the 2019 Conference of the North American Chapter of the Association for Computational Linguistics: Human Language Technologies, Volume 1 (Long and Short Papers)*, pages 4171–4186, Minneapolis, Minnesota, June 2019. Association for Computational Linguistics.
- [12] Emilien Dupont, Arnaud Doucet, and Yee Whye Teh. Augmented neural odes. In H. Wallach, H. Larochelle, A. Beygelzimer, F. d’Alché-Buc, E. Fox, and R. Garnett, editors, *Advances in Neural Information Processing Systems*, volume 32. Curran Associates, Inc., 2019.
- [13] Amirata Ghorbani, Abubakar Abid, and James Zou. Interpretation of neural networks is fragile. *Proceedings of the AAAI Conference on Artificial Intelligence*, 33(01):3681–3688, Jul. 2019.

[14] Ole-Christoffer Granmo. The Tsetlin Machine - A Game Theoretic Bandit Driven Approach to Optimal Pattern Recognition with Propositional Logic. *arXiv preprint arXiv:1804.01508*, 2018.

[15] Ole-Christoffer Granmo, Sondre Glimsdal, Lei Jiao, Morten Goodwin, Christian W. Omlin, and Geir Thore Berge. The Convolutional Tsetlin Machine. *arXiv preprint arXiv:1905.09688*, 2019.

[16] Sarthak Jain and Byron C. Wallace. Attention is not Explanation. In *Proceedings of the 2019 Conference of the North American Chapter of the Association for Computational Linguistics: Human Language Technologies, Volume 1 (Long and Short Papers)*, pages 3543–3556, Minneapolis, Minnesota, June 2019. Association for Computational Linguistics.

[17] Kai Jia and Martin Rinard. Efficient exact verification of binarized neural networks. In H. Larochelle, M. Ranzato, R. Hadsell, M. F. Balcan, and H. Lin, editors, *Advances in Neural Information Processing Systems*, volume 33, pages 1782–1795. Curran Associates, Inc., 2020.

[18] Lei Jiao, Xuan Zhang, Ole-Christoffer Granmo, and K Darshana Abeyrathna. On the Convergence of Tsetlin Machines for the XOR Operator. *arXiv preprint arXiv:2101.02547*, 2021.

[19] Alex Krizhevsky, Geoffrey Hinton, et al. Learning multiple layers of features from tiny images. 2009.

[20] Yann LeCun and Corinna Cortes. MNIST handwritten digit database. 2010.

[21] Jie Lei, Tousif Rahman, Rishad Shafik, Adrian Wheeldon, Alex Yakovlev, Ole-Christoffer Granmo, Fahim Kawsar, and Akhil Mathur. Low-Power Audio Keyword Spotting Using Tsetlin Machines. *Journal of Low Power Electronics and Applications*, 11, 2021.

[22] Zeyang Lei, Yujiu Yang, Min Yang, Wei Zhao, Jun Guo, and Yi Liu. A human-like semantic cognition network for aspect-level sentiment classification. *Proceedings of the AAAI Conference on Artificial Intelligence*, 33(01):6650–6657, Jul. 2019.

[23] Qian Liu, Heyan Huang, Yang Gao, Xiaochi Wei, Yuxin Tian, and Luyang Liu. Task-oriented word embedding for text classification. In *Proceedings of the 27th International Conference on Computational Linguistics*, pages 2023–2032, Santa Fe, New Mexico, USA, August 2018.

[24] Rosanne Liu, Joel Lehman, Piero Molino, Felipe Petroski Such, Eric Frank, Alex Sergeev, and Jason Yosinski. An intriguing failing of convolutional neural networks and the coordconv solution. In *Proceedings of the 32Nd International Conference on Neural Information Processing Systems*, NIPS’18, pages 9628–9639, 2018.

[25] Andrew L. Maas, Raymond E. Daly, Peter T. Pham, Dan Huang, Andrew Y. Ng, and Christopher Potts. Learning word vectors for sentiment analysis. In *Proceedings of the 49th Annual Meeting of the Association for Computational Linguistics: Human Language Technologies*, pages 142–150, Portland, Oregon, USA, June 2011. Association for Computational Linguistics.

[26] Abinaya Manimaran, Thiagarajan Ramanathan, Suya You, and C.-C. Jay Kuo. Visualization, discriminability and applications of interpretable saak features. *CoRR*, abs/1902.09107, 2019.

[27] Nina Narodytska, Shiva Kasiviswanathan, Leonid Ryzhyk, Mooly Sagiv, and Toby Walsh. Verifying properties of binarized deep neural networks. In *Proceedings of the AAAI Conference on Artificial Intelligence*, volume 32, 2018.

[28] I. Noveck, R. B. Lea, George M. Davidson, and D. O’brien. Human reasoning is both logical and pragmatic. *Intellectica*, 11:81–109, 1991.

[29] Matthew Peters, Mark Neumann, Mohit Iyyer, Matt Gardner, Christopher Clark, Kenton Lee, and Luke Zettlemoyer. Deep contextualized word representations. In *Proceedings of the 2018 Conference of the North American Chapter of the Association for Computational Linguistics: Human Language Technologies, Volume 1 (Long Papers)*, pages 2227–2237, New Orleans, Louisiana, June 2018. Association for Computational Linguistics.

[30] Adityanarayanan Radhakrishnan, Charles Durham, Ali Soylemezoglu, and Caroline Uhler. Patchnet: Interpretable neural networks for image classification, 2018.

[31] H. Robbins. A stochastic approximation method. *Annals of Mathematical Statistics*, 22:400–407, 2007.

[32] Cynthia Rudin. Stop explaining black box machine learning models for high stakes decisions and use interpretable models instead. *Nature Machine Intelligence*, 1, 2019.

[33] Ramprasaath R. Selvaraju, Michael Cogswell, Abhishek Das, Ramakrishna Vedantam, Devi Parikh, and Dhruv Batra. Grad-cam: Visual explanations from deep networks via gradient-based localization. In *2017 IEEE International Conference on Computer Vision (ICCV)*, pages 618–626, 2017.

[34] Sofia Serrano and Noah A. Smith. Is attention interpretable? In *Proceedings of the 57th Annual Meeting of the Association for Computational Linguistics*, pages 2931–2951, Florence, Italy, July 2019. Association for Computational Linguistics.

[35] Karen Simonyan, Andrea Vedaldi, and Andrew Zisserman. Deep inside convolutional networks: Visualising image classification models and saliency maps, 2014.

[36] Richard Socher, Alex Perelygin, Jean Wu, Jason Chuang, Christopher D. Manning, Andrew Ng, and Christopher Potts. Recursive deep models for semantic compositionality over a sentiment treebank. In *Proceedings of the 2013 Conference on Empirical Methods in Natural Language Processing*, pages 1631–1642, Seattle, Washington, USA, October 2013. Association for Computational Linguistics.

[37] Nitish Srivastava, Geoffrey Hinton, Alex Krizhevsky, Ilya Sutskever, and Ruslan Salakhutdinov. Dropout: A simple way to prevent neural networks from overfitting. *Journal of Machine Learning Research*, 15(56):1929–1958, 2014.

[38] Xiaobing Sun and Wei Lu. Understanding attention for text classification. In *Proceedings of the 58th Annual Meeting of the Association for Computational Linguistics*, pages 3418–3428, Online, July 2020. Association for Computational Linguistics.

[39] Amirhossein Tavanaei. Embedded encoder-decoder in convolutional networks towards explainable ai, 2020.

[40] Leslie G Valiant. A Theory of the Learnable. *Communications of the ACM*, 27(11):1134–1142, 1984.

[41] Peng Xu, Andrea Madotto, Chien-Sheng Wu, Ji Ho Park, and Pascale Fung. Emo2Vec: Learning generalized emotion representation by multi-task training. In *Proceedings of the 9th Workshop on Computational Approaches to Subjectivity, Sentiment and Social Media Analysis*, pages 292–298, Brussels, Belgium, October 2018. Association for Computational Linguistics.

[42] Rohan Kumar Yadav, Lei Jiao, Ole-Christoffer Granmo, and Morten Goodwin. Distributed Word Representation in Tsetlin Machine. *arXiv preprint arXiv:2104.06901*, 2021.

[43] Rohan Kumar Yadav, Lei Jiao, Ole-Christoffer Granmo, and Morten Goodwin. Human-Level Interpretable Learning for Aspect-Based Sentiment Analysis. In *The Thirty-Fifth AAAI Conference on Artificial Intelligence (AAAI-21)*. AAAI, 2021.

[44] Rohan Kumar Yadav, Lei Jiao, Ole-Christoffer Granmo, and Morten Goodwin. Human-Level Interpretable Learning for Aspect-Based Sentiment Analysis. In *The Thirty-Fifth AAAI Conference on Artificial Intelligence (AAAI-21)*. AAAI, 2021.

[45] Quanshi Zhang, Ying Nian Wu, and Song-Chun Zhu. Interpretable convolutional neural networks. In *Proceedings of the IEEE Conference on Computer Vision and Pattern Recognition*, pages 8827–8836, 2018.

[46] Xuan Zhang, Lei Jiao, Ole-Christoffer Granmo, and Morten Goodwin. On the Convergence of Tsetlin Machines for the IDENTITY-and NOT Operators. *arXiv preprint arXiv:2007.14268*, 2020.

A Appendix

A.1 Tsetlin Machine

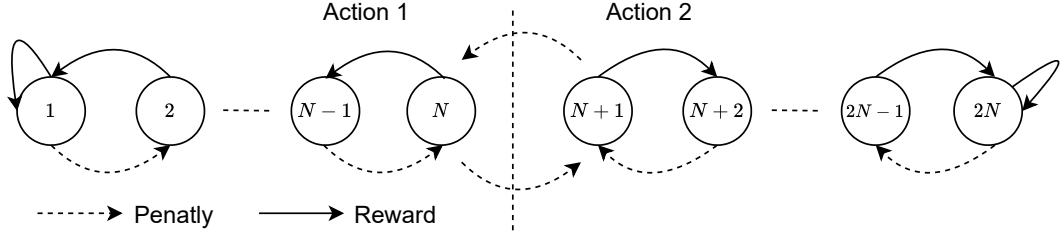


Figure 5: A two-action Tsetlin Automaton with $2N$ states.

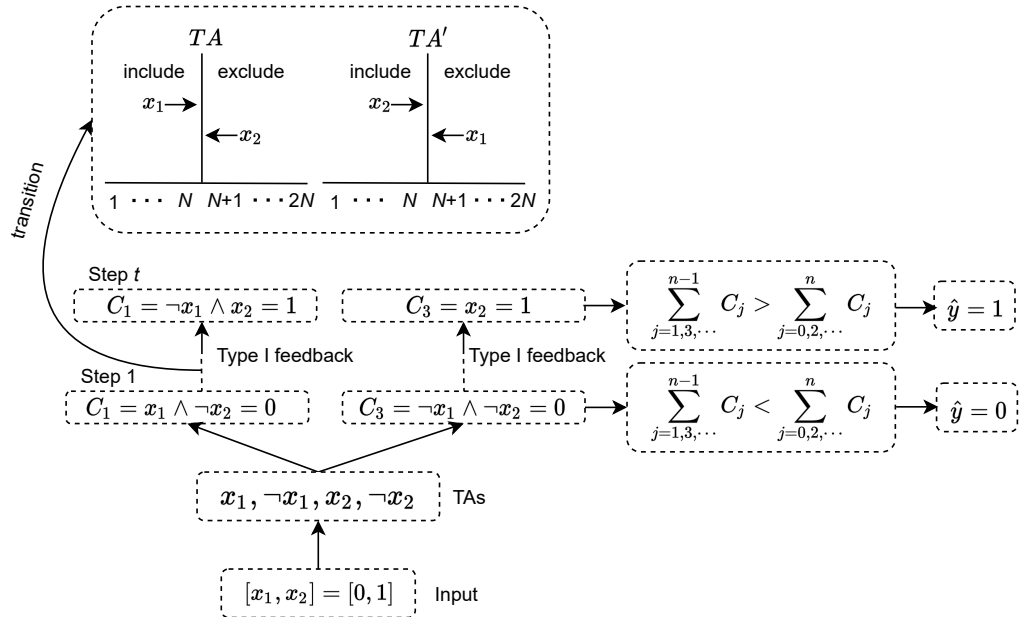


Figure 6: TM learning dynamics for an XOR-gate training sample, with input $(x_1 = 0, x_2 = 1)$ and output target $y = 1$.

Structure. A TM in its simplest form takes a feature vector $\mathbf{x} = [x_1, x_2, \dots, x_o] \in \{0, 1\}^o$ of o propositional values as input and assigns the vector a class $\hat{y} \in \{0, 1\}$. To minimize classification error, the TM produces n self-contained patterns. In brief, the input vector \mathbf{x} provides the literal set $L = \{l_1, l_2, \dots, l_{2o}\} = \{x_1, x_2, \dots, x_o, \neg x_1, \neg x_2, \dots, \neg x_o\}$, consisting of the input features and their negations. By selecting subsets $L_j \subseteq L$ of the literals, the TM can build arbitrarily complex patterns, ANDing the selected literals to form conjunctive clauses:

$$C_j(\mathbf{x}) = \bigwedge_{l_k \in L_j} l_k. \quad (4)$$

Above, $j \in \{1, 2, \dots, n\}$ refers to a particular clause C_j and $k \in \{1, 2, \dots, 2o\}$ refers to a particular literal l_k . As an example, the clause $C_j(\mathbf{x}) = x_1 \wedge \neg x_2$ consists of the literals $L_j = \{x_1, \neg x_2\}$ and evaluates to 1 when $x_1 = 1$ and $x_2 = 0$.

The TM assigns one TA per literal l_k per clause C_j to build the clauses. The TA assigned to literal l_k of clause C_j decides whether l_k is *Excluded* or *Included* in C_j . Figure 5 depicts a two-action TA with $2N$ states. For states 1 to N , the TA performs action *Exclude* (Action 1), while for states $N+1$ to $2N$, it performs action *Include* (Action 2).

INPUT	CLAUSE LITERAL	1		0	
		1	0	1	0
INCLUDE LITERAL	P(REWARD)	$\frac{s-1}{s}$	NA	0	0
	P(INACTION)	$\frac{1}{s}$	NA	$\frac{s-1}{s}$	$\frac{s-1}{s}$
	P(PENALTY)	0	NA	$\frac{1}{s}$	$\frac{1}{s}$
EXCLUDE LITERAL	P(REWARD)	0	$\frac{1}{s}$	$\frac{1}{s}$	$\frac{1}{s}$
	P(INACTION)	$\frac{1}{s}$	$\frac{s-1}{s}$	$\frac{s-1}{s}$	$\frac{s-1}{s}$
	P(PENALTY)	$\frac{s-1}{s}$	0	0	0

Table 5: Type I Feedback

INPUT	CLAUSE LITERAL	1		0	
		1	0	1	0
INCLUDE LITERAL	P(REWARD)	0	NA	0	0
	P(INACTION)	1.0	NA	1.0	1.0
	P(PENALTY)	0	NA	0	0
EXCLUDE LITERAL	P(REWARD)	0	0	0	0
	P(INACTION)	1.0	0	1.0	1.0
	P(PENALTY)	0	1.0	0	0

Table 6: Type II Feedback

to $2N$ it performs action *Include* (Action 2). As feedback to the action performed, the environment responds with either a Reward or a Penalty. If the TA receives a Reward, it moves deeper into the side of the action. If it receives a Penalty, it moves towards the middle and eventually switches action.

With n clauses and $2o$ literals, we get $n \times 2o$ TAs. We organize the states of these in a $n \times 2o$ matrix $A = [a_k^j] \in \{1, 2, \dots, 2N\}^{n \times 2o}$. We will use the function $g(\cdot)$ to map the automaton state a_k^j to Action 0 (*Exclude*) for states 1 to N and to Action 1 (*Include*) for states $N + 1$ to $2N$: $g(a_k^j) = a_k^j > N$.

We can connect the states a_k^j of the TAs assigned to clause C_j with its composition as follows:

$$C_j(\mathbf{x}) = \bigwedge_{l_k \in L_j} l_k = \bigwedge_{k=1}^{2o} \left[g(a_k^j) \Rightarrow l_k \right]. \quad (5)$$

Here, l_k is one of the literals and a_k^j is the state of its TA in clause C_j . The logical *imply* operator \Rightarrow implements the *Exclude/Include* action. That is, the *imply* operator is always 1 if $g(a_k^j) = 0$ (*Exclude*), while if $g(a_k^j) = 1$ (*Include*) the truth value is decided by the truth value of the literal.

Classification. Classification is performed as a majority vote. The odd-numbered half of the clauses vote for class $\hat{y} = 0$ and the even-numbered half vote for $\hat{y} = 1$:

$$\hat{y} = 0 \leq \sum_{j=1,3,\dots}^{n-1} \bigwedge_{k=1}^{2o} \left[g(a_k^j) \Rightarrow l_k \right] - \sum_{j=2,4,\dots}^n \bigwedge_{k=1}^{2o} \left[g(a_k^j) \Rightarrow l_k \right]. \quad (6)$$

As such, the odd-numbered clauses have positive polarity, while the even-numbered ones have negative polarity. As an example, consider the input vector $\mathbf{x} = [0, 1]$ in the lower part of Figure 6. The figure depicts two clauses of positive polarity, $C_1(\mathbf{x}) = x_1 \wedge \neg x_2$ and $C_3(\mathbf{x}) = \neg x_1 \wedge \neg x_2$ (the negative polarity clauses are not shown). Both of the clauses evaluate to zero, leading to class prediction $\hat{y} = 0$.

Learning. The upper part of Figure 6 illustrates learning. A TM learns online, processing one training example (\mathbf{x}, y) at a time. Based on (\mathbf{x}, y) , the TM rewards and penalizes its TAs, which amounts to incrementing and decrementing their states. There are two kinds of feedback: Type I Feedback produces frequent patterns and Type II Feedback increases the discrimination power of the patterns.

Type I feedback is given stochastically to clauses with positive polarity when $y = 1$ and to clauses with negative polarity when $y = 0$. Conversely, Type II Feedback is given stochastically to clauses with positive polarity when $y = 0$ and to clauses with negative polarity when $y = 1$. The probability of a clause being updated is based on the vote sum v : $v = \sum_{j=1,3,\dots}^{n-1} \bigwedge_{k=1}^{2o} \left[g(a_k^j) \Rightarrow l_k \right] - \sum_{j=2,4,\dots}^n \bigwedge_{k=1}^{2o} \left[g(a_k^j) \Rightarrow l_k \right]$. The voting error is calculated as:

$$\epsilon = \begin{cases} T - v & y = 1 \\ T + v & y = 0. \end{cases} \quad (7)$$

Here, T is a user-configurable voting margin yielding an ensemble effect. The probability of updating each clause is $P(\text{Feedback}) = \frac{\epsilon}{2T}$.

After random sampling from $P(\text{Feedback})$ has decided which clauses to update, the following TA state updates can be formulated as matrix additions, subdividing Type I Feedback into feedback Type Ia and Type Ib:

$$A_{t+1}^* = A_t + F^{II} + F^{Ia} - F^{Ib}. \quad (8)$$

Here, $A_t = [a_k^j] \in \{1, 2, \dots, 2N\}^{n \times 2o}$ contains the states of the TAs at time step t and A_{t+1}^* contains the updated state for time step $t+1$ (before clipping). The matrices $F^{Ia} \in \{0, 1\}^{n \times 2o}$ and $F^{Ib} \in \{0, 1\}^{n \times 2o}$ contains Type I Feedback. A zero-element means no feedback and a one-element means feedback. As shown in Table 5, two rules govern Type I feedback:

- **Type Ia Feedback** is given with probability $\frac{s-1}{s}$ whenever both clause and literal are 1-valued.³ It penalizes *Exclude* actions and rewards *Include* actions. The purpose is to remember and refine the patterns manifested in the current input \mathbf{x} . This is achieved by increasing selected TA states. The user-configurable parameter s controls pattern frequency, i.e., a higher s produces less frequent patterns.
- **Type Ib Feedback** is given with probability $\frac{1}{s}$ whenever either clause or literal is 0-valued. This feedback rewards *Exclude* actions and penalizes *Include* actions to coarsen patterns, combating overfitting. Thus, the selected TA states are decreased.

The matrix $F^{II} \in \{0, 1\}^{n \times 2o}$ contains Type II Feedback to the TAs, given per Table 6.

- **Type II Feedback** penalizes *Exclude* actions to make the clauses more discriminative, combating false positives. That is, if the literal is 0-valued and the clause is 1-valued, TA states below $N+1$ are increased. Eventually the clause becomes 0-valued for that particular input, upon inclusion of the 0-valued literal.

The final updating step for training example (\mathbf{x}, y) is to clip the state values to make sure that they stay within value 1 and $2N$:

$$A_{t+1} = \text{clip}(A_{t+1}^*, 1, 2N). \quad (9)$$

For example, both of the clauses in Figure 6 receives Type I Feedback over several training examples, making them resemble the input associated with $y = 1$.

A.2 Convolutional Tsetlin Machine

Consider a set of images $\mathcal{X} = \{\mathbf{x}_e | 1 \leq e \leq E\}$, where e is the index of the images. Each image is of size $d_x \times d_y$ and consists of d_z binary layers, illustrated in Figure 8b. A classic TM models such an image with an input vector $\mathbf{x} = [x_k] \in \{0, 1\}^{d_x \times d_y \times d_z}$ that contains $d_x \times d_y \times d_z$ input features. Accordingly, each clause is composed from $d_x \times d_y \times d_z \times 2$ literals.

³Note that the probability $\frac{s-1}{s}$ is replaced by 1 when boosting true positives.

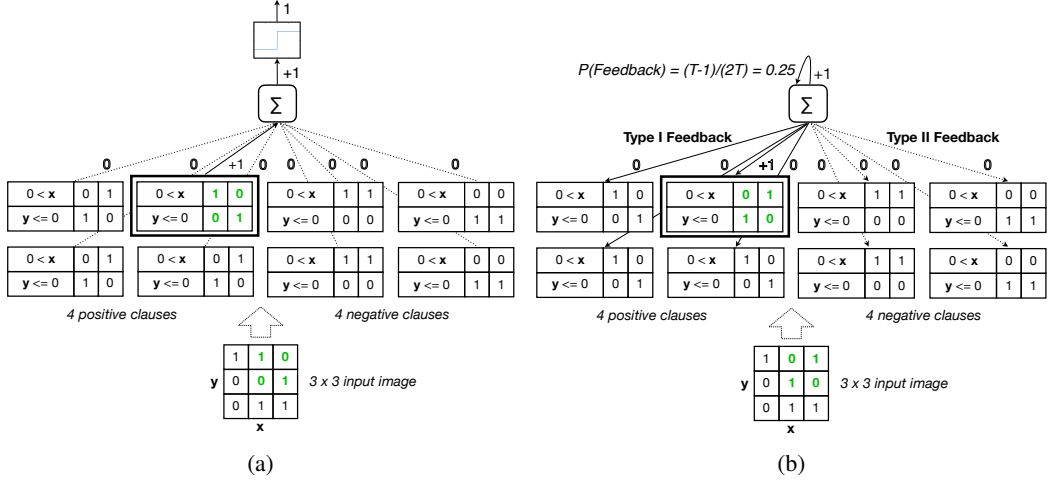


Figure 7: Example of inference (a) and learning (b) for the Noisy 2D XOR Problem.

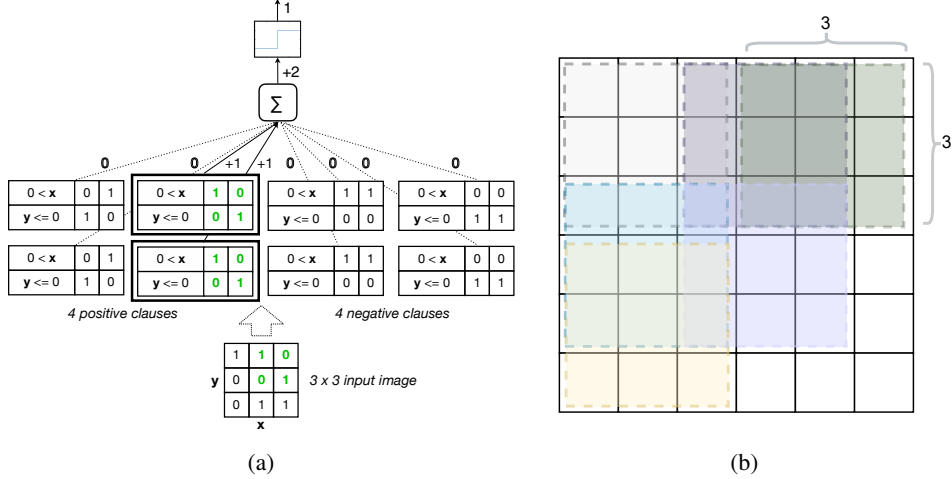


Figure 8: (a) Goal state for the Noisy 2D XOR Problem. (b) Illustration of image, filter and patches.

Structure. The CTM (CTM) [15] performs a convolution over the input image \mathbf{x} , dividing it into patches with spatial dimensions $d_w \times d_w$. That is, the input vector $\mathbf{x} = [x_k] \in \{0, 1\}^{d_x \times d_y \times d_z}$ produces $B = \left(\left\lceil \frac{d_x - d_w}{q} \right\rceil + 1\right) \times \left(\left\lceil \frac{d_y - d_w}{q} \right\rceil + 1\right)$ patches, with q being the step size of the convolution. For instance, Figure 8b illustrates $B = (6 - 3 + 1) \times (6 - 3 + 1) = 16$ patches of size 3×3 , assuming step size $q = 1$.

Each patch $b \in \{1, 2, \dots, B\}$, in turn, yields an input vector $\mathbf{x}^b = [x_k^b] \in \{0, 1\}^{d_w \times d_w \times d_z}$ with a corresponding literal vector $\mathbf{l}^b = [l_k^b] \in \{0, 1\}^{d_w \times d_w \times d_z \times 2}$. The CTM becomes location aware [24] by augmenting each patch input vector \mathbf{x}^b with the coordinates of \mathbf{x}^b within \mathbf{x} , using threshold-based encoding [1].

Classification. The CTM is based on the classic TM procedure for classification (Eqn. 6). However, we now have B input vectors \mathbf{x}^b per image rather than a single input vector \mathbf{x} . The convolution is performed by evaluating each clause C_j on each input vector \mathbf{x}^b , i.e., calculating $\bigwedge_{k=1}^{2o} [g(a_k^j) \Rightarrow l_k^b]$, and then ORing the evaluations per clause:

$$\hat{y} = 0 \leq \sum_{j=1,3,\dots}^{n-1} \bigvee_{b=1}^B \left[\bigwedge_{k=1}^{2o} [g(a_k^j) \Rightarrow l_k^b] \right] - \sum_{j=2,4,\dots}^n \bigvee_{b=1}^B \left[\bigwedge_{k=1}^{2o} [g(a_k^j) \Rightarrow l_k^b] \right]. \quad (10)$$

Figure 7a provides an example where a 3×3 input image produces four 2×2 patches. The CTM has four clauses of positive polarity and four clauses of negative polarity. Only one of the clauses of positive polarity matches. This clause matches the upper left corner of the input image, hence evaluating to 1. Accordingly, the net output sum is +1, yielding output $\hat{y} = 1$.

Learning. CTM learning leverages the TM learning procedure, per Eqn. 8 and Eqn. 9. However, when giving Type Ia or Type II Feedback to each clause C_j , the CTM does not use the original input vector \mathbf{x} . Instead, it randomly selects one of the patch input vectors \mathbf{x}^b that made the clause evaluate to 1:

$$\mathbf{x}_j^b = \text{RandomChoice} \left(\left\{ \mathbf{x}^b \left| \bigwedge_{k=1}^{2o} \left[g(a_k^j) \Rightarrow l_k^b \right] = 1, 1 \leq b \leq B \right. \right\} \right). \quad (11)$$

For Type Ib Feedback, on the other hand, CTM follows the standard updating scheme.

The reason for randomly selecting a patch input vector \mathbf{x}^b is to have each clause extract a certain sub-pattern, and the randomness of the uniform distribution statistically spreads the clauses for different sub-patterns in the target image.

Figure 7b demonstrates a learning step. Only a single clause has recognized the input. Assuming a summation target (margin) of $T = 2$ and net clause output sum +1 the probability of giving each clause feedback becomes $P(\text{Feedback}) = \frac{(2-1)}{2^2} = 0.25$. Since the training example is $y = 1$, the positive polarity clauses receives Type I Feedback with probability 0.25, while the negative polarity clauses receive Type II feedback again with probability 0.25. After several such updates, we have a more balanced representation of the input patterns in Figure 8a, with two clauses now recognizing the input.

A.3 Convergence Insights

It is analyzed in [46] and [18] for the convergence properties of the vanilla TM for 1-bit case and XOR case respectively. Here we will briefly analyse the impact of the introduced randomized clause drop on the convergence. For the 1-bit case, the work in [46] is to study the convergence feature of a TM with only one clause. When the randomized clause drop proposed is adopted, it will not influence the conclusions drawn in [46] and the reasons are as follows. The main difference between the proposed algorithm and the vanilla TM is that the clause in this work will not be updated upon each given training sample, but according to a pre-defined probability. In other words, the clause is updated based on a randomly down-sampled subset as a new training set compared with the original training data. Given infinite training data and ideally randomized down-sampling, the statistics of the samples in the subset is kept the same as the original training data set and the number of training samples is also sufficient. For this reason, the clause can still observe sufficient number of training samples and can also observe sufficient varieties of the training samples. In addition, the other updating rules are unchanged compared with the vanilla TM. Therefore, all conclusions in [46] hold for the newly proposed algorithm.

For the XOR case, there are two sub-patterns in the XOR operator and the TM is proven to be able to converge and learn both sub-patterns when threshold value T is correctly configured [18]. According to the analysis in the previous paragraph, we understand that the training samples for the new algorithm is a down-sampled version of the original data set and the statistics of the samples is kept the same due to the ideal randomness. If the training samples with only one sub-pattern are given, the randomized down sampled data, given infinite time horizon, will still offer sufficient samples with the same probability distribution compared with the original training set. Therefore, Lemma 1 and Lemma 2 in [18] hold. In fact, when the training samples with both sub-patterns are given, Lemma 3 and Lemma 4 in [18] still hold. The reason is that ideal randomly down-sampling will not make the new training data biased in terms of the sub-patterns and thus will not change the nature of the recurrence for the clauses. Clearly, Lemma 5 in [18] is also true because the newly introduced process will not change the role of T . Theorem 2 in [18] is therefore self-evident. Indeed, the conclusion derived in [18] is applicable to the algorithm with drop clause.